

Trapping of light by metal arrays

This article has been downloaded from IOPscience. Please scroll down to see the full text article.

2010 J. Opt. 12 045102

(<http://iopscience.iop.org/2040-8986/12/4/045102>)

[The Table of Contents](#) and [more related content](#) is available

Download details:

IP Address: 194.44.7.8

The article was downloaded on 26/03/2010 at 06:28

Please note that [terms and conditions apply](#).

Trapping of light by metal arrays

Vyacheslav V Khardikov^{1,2}, Ekaterina O Iarko¹ and
Sergey L Prosvirnin^{1,2,3}

¹ Institute of Radio Astronomy, Kharkiv 61002, Ukraine

² School of Radio Physics, Karazin Kharkiv National University, Kharkiv 61077, Ukraine

E-mail: khardikov@univer.kharkov.ua, yarkokatya@rian.kharkov.ua (E O Iarko) and
prosvirn@rian.kharkov.ua

Received 13 November 2009, accepted for publication 18 February 2010

Published 25 March 2010

Online at stacks.iop.org/JOpt/12/045102

Abstract

The problem of the near-IR light reflection from and transmittance through a planar 2D periodic metal–dielectric structure with a square periodic cell of two complex-shaped asymmetric metal elements has been solved. Conditions of the light confinement by excitation of the trapped mode resonances in certain structures, both polarization-sensitive and polarization-insensitive, were studied. For the first time, the existence of a high-order trapped mode resonance with the greater quality factor than that of the lowest one has been shown. It was ascertained that the Babinet principle provides a good prediction of the resonance properties of the complementary structures, despite the very high Joule losses in the metal strips in near-IR, a finite thickness of the metal elements and the presence of a dielectric substrate.

Keywords: array, diffraction, reflection, trapped mode, resonance, metamaterials

(Some figures in this article are in colour only in the electronic version)

1. Introduction

One-periodic planar arrays of straight wires or metal strips have a long history of applications as quasi-optical polarizing devices. Their properties are well known.

Planar double-periodic structures have been used in the microwave, terahertz and optical frequency ranges because of their manufacturing simplicity and the many remarkable electromagnetic properties of such surfaces. In microwaves, these structures are used as absorbing and scattering covers, and frequency-selective and polarization-selective surfaces [1]. Planar periodic structures of complex-shaped metal strips have features of resonance transmission and reflection of incident waves without any high diffraction orders forming. Thus, they are the basis for a series of artificial materials including metamaterials. They are at the heart of such promising modern scientific branches as the creation of artificial magnetic and double-negative media [2], layers with asymmetric light transmission [3, 4], ‘invisible’ metals [5], high-impedance surfaces with the magnetic mirror property [6] and ‘cloaks’ [7], for example. Because of the wide range of outstanding physical properties, the planar double-periodic structures are useful in designing novel devices with unique characteristics

for electromagnetic waves from the microwave to optical range.

Not long ago, the possibility of high-quality factor ‘trapped mode’ resonances in microwave planar periodic structures was shown theoretically [8, 9], then studied in [10] and confirmed experimentally [11]. The zero-reflection response from a dipole array with an element perturbation where every second element has a different resonant frequency was studied in [12] as a distortion factor of the dual-bandstop FSS responses.

These trapped mode resonances are excited in planar double-periodic structures with at least two metal strips in a periodic cell. A small asymmetry of the metal elements of such structures results in excitation of the strong anti-phased current modes through a weak free-space coupling, which provides low radiation losses and therefore high Q -factor resonances in microwaves. Such types of resonances are very important in the optical range, where a high level of energy dissipation in the metal elements of the structure and large radiation losses cause a low-quality factor of ordinary resonances.

The main feature that distinguishes the trapped mode resonance from the ordinary dimensional resonance of periodic structures is that its eigenfrequency may be real on the assumption of infinitesimal dissipation of the structure,

³ <http://prosvirn.uaic.net>

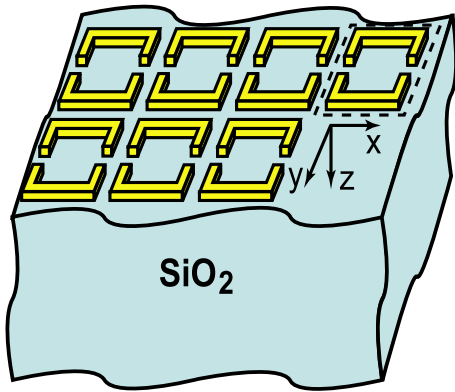


Figure 1. A typical planar double-periodic structure composed of an array of C-shaped metal elements placed on a silica substrate. A periodic cell of the array is shown by a dashed line.

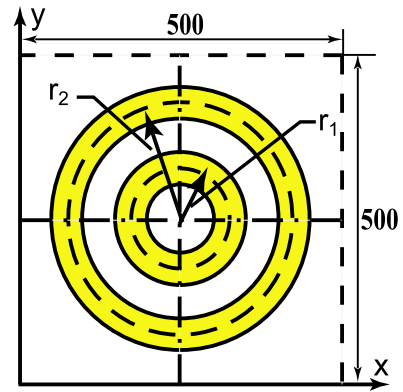


Figure 2. Square periodic cell of planar array of paired concentric rings. Radii r_1 and r_2 are the medial radii of inner and outer concentric rings. The sizes are shown in nanometers.

i.e. radiation losses may be zero. As a result, the quality factor of this resonance is higher than the ordinary one. The wavelength dependence of the resonance reflection response has a typical peak-and-trough, so-called Fano, profile [13], resulting from the excitation of a localized field of the trapped mode with a discrete spectrum.

The planar structures with the trapped mode resonance are very promising for applications. For example, due to greatly increasing electric fields near the structure in the trapped mode resonance regime, the structure can be effectively used as a biosensor. Another perspective application is a ‘lasing spacer’, which was proposed in [14]. The lasing spacer is a planar source of spatially and temporally coherent radiation which consists of a planar double-periodic structure in the trapped mode resonance regime and a thin substrate of a gain medium.

A recent paper [15] demonstrated, for the first time, experimental evidence of the compensation of Joule losses in a metallic photonic planar structure using a layer of semiconductor quantum dots. It opens up the intriguing possibility of double-periodic planar structure applications for optical range metamaterials. However, it requires additional study of the trapped mode resonance in split structures, which are complementary to the wire structures. In the strict sense, the Babinet principle is only applicable in problems of electromagnetic wave diffraction by complementary infinitely thin and perfect conducting plane metal screens. There are some factors which result in the inapplicability of the Babinet principle to directly convert one problem’s solution to the solution of a corresponding complementary problem. The first of them is a finite thickness of the screen with slits and wires. The second one is a structural asymmetry which is conditioned by the presence of a dielectric substrate. The third factor is a finite conductivity of the structural metal in the infrared and optical ranges.

Thus, the use of a planar structure with ‘trapped mode’ resonance is very useful in the infrared and optical ranges. In fact, we observe the effect of light trapping by metal arrays with a high level of IR power stored in localized field states of the discrete spectrum. However due to a strong dissipation and dispersion of the metal permittivity in these ranges, there is an acute need for a detailed study of the excitation and other

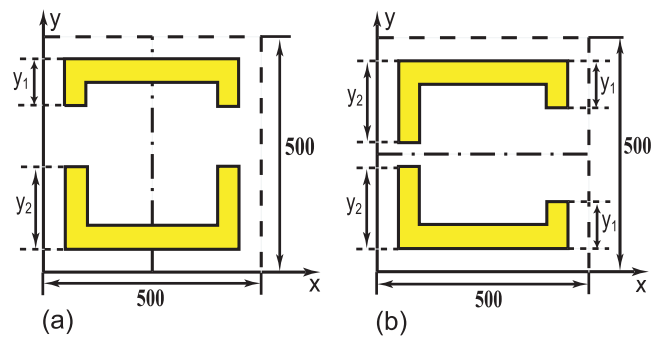


Figure 3. Square periodic cells of planar arrays consisted of asymmetrically broken square frames. The cell (a) consists of two symmetric C-shaped elements which have different lengths. Two identical asymmetric C-shaped elements of the cell (b) have the same lengths. Metal elements of both kinds of periodic cells are formed from a square frame with the length of side 400 nm. The sizes are shown in nanometers.

properties of the trapped mode resonances in planar double-periodic structures for optical and infrared applications. In this paper we present the results of our theoretical study of the main features of trapped mode resonances in some kinds of structures in the near-IR range.

2. Problem statement and method of solution

A typical planar structure composed of an array of C-shaped metal strips placed on a transparent substrate is shown in figure 1. The periodic cells of the arrays under consideration include a pair of complex-shaped metal elements of a similar shape but different lengths. In this study, we consider arrays consisting of paired concentric rings (figure 2) and asymmetric C-shaped metal elements (figure 3). The axes of symmetry of the array are shown by the dashed–dotted lines in these figures. A normally incident plane wave polarized transversely to the array symmetry axis can excite the trapped mode resonances. Thus the trapped mode resonances of the structures in figures 3(a) and (b) can be excited by the incident x - and y -polarized plane waves correspondingly. The fourfold symmetry square periodic cell array of concentric

rings (figure 2) presents an example of a polarization-insensitive structure.

We study the resonance responses of the arrays in the near-infrared wavelength region from 750 to 3000 nm. Periodic cells of all the structures were chosen as square shapes with sizes $d_x = d_y = 500$ nm. We assume that the strip elements of all kinds of arrays have rectangular cross sections of the same thickness and a width of 50 nm. The thickness of the substrate is L . The metal of the strips is assumed to be gold or aluminum, and the substrate material is synthetic fused silica (amorphous silicon dioxide).

The solution of the problem of electromagnetic wave diffraction by double-periodic planar arrays composed of paired coupled metal elements serves as a basis to analyze the trapped mode resonances in the infrared range. The resonance sizes and a complex shape of the elements of the arrays, a strong dispersion of the metals and a high level of dissipative losses cause the use of numerical methods of wave diffraction theory.

Time domain numerical methods are widely used for such kinds of problems, because they afford the opportunity to calculate the reflection and transmission coefficients in the whole wavelength range of interest for one numerical simulation. In this study, we use the mapped pseudo-spectral time domain (PSTD) method [16].

The generally known Fourier PSTD method uses uniformly located collocation points and Fourier series as basis functions. It enables us to derive a simple expression for the spatial derivatives of the fields without a spatial dispersion error which is inherent in the traditional FDTD algorithm. As a result, the PSTD method requires much less internal memory and computation time to solve 3D diffraction problems than the FDTD method.

Unfortunately, over the Gibbs phenomenon, the Fourier PSTD method is only a first-order accuracy numerical method as applied to the solution of the problems of electromagnetic wave diffraction by the structures that include interfaces between high-contrast materials. The algorithm can be improved by using a nonuniform mesh concentrated close to the interfaces. Due to the use of a conformed nonuniform mesh, the mapped PSTD method [16] provides an effective decrease of the Gibbs phenomenon at the high-contrast materials' interfaces over the whole wavelength range of interest. Fast Fourier transform (FFT) and a mapping curve of a special form are used to calculate the spatial field derivatives at collocation points. For example, at the nodes $(x_n)_{n=1}^N$ of a nonuniform mesh constructed in real space, the derivative of the function $f(x)$ is calculated by the following algorithm:

$$\frac{d}{dx} f(x_n) = \frac{df(u_n)/du}{(dx/du)_n} = \frac{(\text{IFFT}(ik_m \text{FFT}(f(u_n))))}{(dx/du)_n} \quad (1)$$

where FFT and IFFT are direct and inverse FFT, respectively, $k_m = 2\pi m/d_x$, ($m = 0, 1, 2, \dots, N - 1$), d_x is the period of the structure along the x direction, $(u_n)_{n=1}^N$ are nodes of an uniform mesh and $x(u)$ is a mapping curve, i.e. a specially constructed smooth curve to map the nonuniform mesh onto a uniform one. The mapping curve provides a very

smooth decrease of the nonuniform mesh spacing at the high-contrast materials' interfaces. Examples of the mapping curve generation are presented in [16, 17].

The mapped PSTD method is effective in solving 3D diffraction problems by the structures whose typical sizes are less than about ten minimal wavelengths, just as in other time domain methods. On the other hand, a typical substrate for real optical array structures has a thickness 0.3–0.5 mm. Thus, the total thickness of the considered structures is thousands of times greater than the minimal wavelength inside the substrate dielectric. The mapped PSTD method is absolutely ineffective in this case. Earlier, we proposed a method to avoid the difficulty of the numerical solution of such kinds of diffraction problems and have proved its effectiveness in [17, 18]. Our approach combines the mapped PSTD method and the analytical method of the transfer matrix. We divide the diffraction problem solving into two stages.

The first stage includes a numerical simulation in order to obtain the transfer matrix of a double-periodic array. For this goal, the mapped PSTD method is used to solve the problem of wave diffraction on a layer that contains a periodic array of metal strips and very thin regular layers of free space and the substrate, which are placed above and below the array, respectively. The free space and substrate layers are required to bound the region of the numerical simulation and they include the regions of 'sources' exciting an electromagnetic field and 'probes' for field registration. As a result of this stage of the problem solution, we calculate a transfer matrix of the above-mentioned array layer.

In the second stage, we multiply the transfer matrix of the array by a preliminary analytically derived transfer matrix of the substrate. The result of the multiplication yields a transfer matrix for the whole metal–dielectric planar structure. This method is very convenient on the assumption that only a zero-order spatial partial wave (Floquet mode) propagates in both free space and the substrate. We assume that all other partial waves are evanescent ones. In the case of a normally incident wave, it requires the satisfaction of the inequality $\max(d_x, d_y) < \lambda/n$ complied in our study, where n is a refractive index of the substrate.

We use the auxiliary differential equation (ADE) technique [19] to take into account the dispersion of the metal and dielectric permittivities. On the assumption that the permittivity dispersion can be approximated by a series of simple frequency functions, this technique lets us consider the media dispersion by introducing some virtual currents. To evaluate the virtual currents, the auxiliary differential equations are formulated in the time domain. These are solved with a PSTD simulation.

In the infrared and optical wavelength ranges, the dispersion dependences of the metal and dielectric permittivities can be approximated by the complex pole model [19] with a very good accuracy. This model of dispersion includes only simple fractional terms, and it is very convenient for using the ADE method. The complex pole model generalizes such high-usage approximations of the dispersion dependences as either conductivity, Drude, or Debye and Lorentz pole models. The approximation of the aluminum permittivity

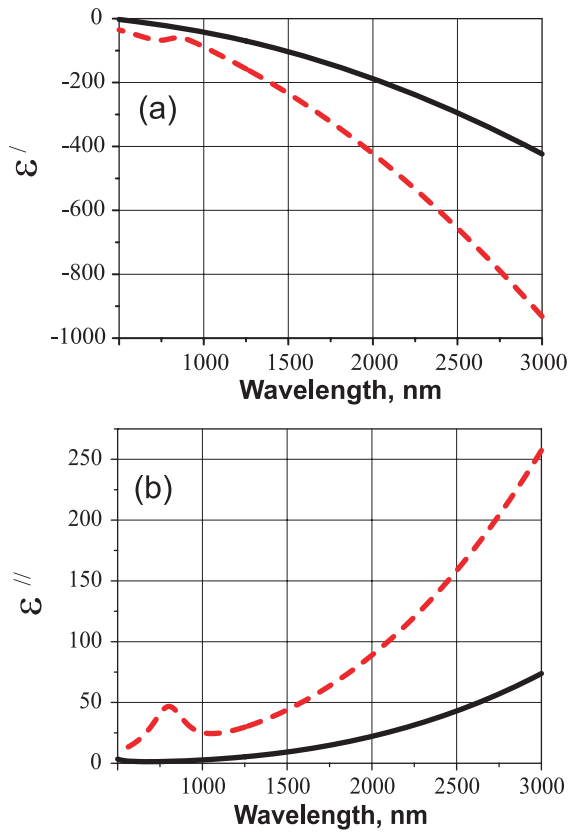


Figure 4. Wavelength dependences of real (a) and imaginary (b) parts of the complex permittivity ($\epsilon = \epsilon' - i\epsilon''$) of gold (solid lines) and aluminum (dashed lines).

dispersion [20] contains the pole model with conductivity, Debye pole pair and three complex poles. We use the model of gold permittivity suggested in [21]. This model includes a Drude pole and complex poles' pair, and it was tested on the solution to the problem of light diffraction by a gold sphere with 80 nm radius in [21]. The wavelength dependences of the gold and aluminum complex permittivity ($\epsilon = \epsilon' - i\epsilon''$) are demonstrated in figure 4. We used the data on refractive index of the synthetic fused silica of the substrate presented in [22].

3. Analysis and discussion of numerical results

At first, for the sake of simplicity, we assume that the metal arrays are placed on a semi-infinite substrate in order to exclude the wave interference resonances inside the substrate. Therefore all the reflection and transmission resonances are produced by the plasmon-polariton resonances of the metal arrays. In a final stage of analysis, we present some data on the substrate finite thickness effect.

3.1. Array of metal strips

Before analyzing the trapped mode resonances in complex structures consisting of asymmetrical metal strips, let us outline the resonance properties of a double-periodic planar structure with an initial one-element periodic cell.

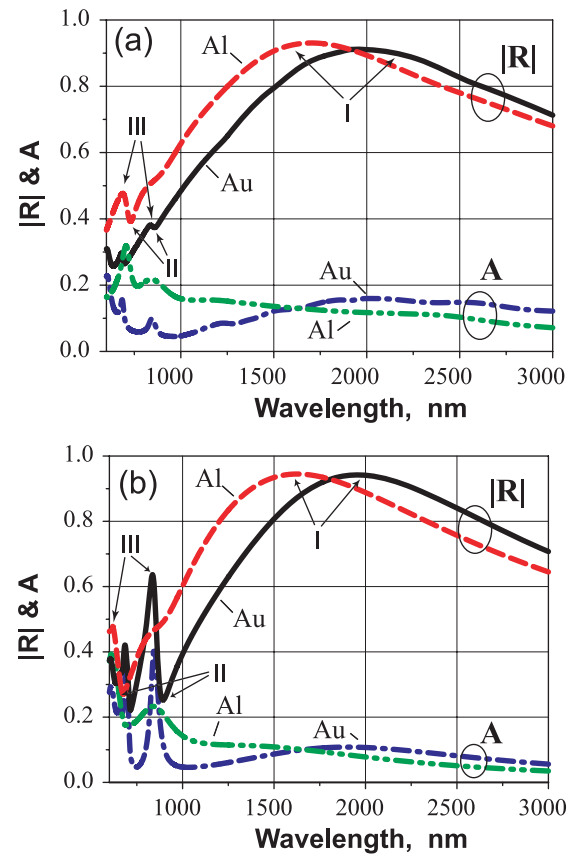


Figure 5. Wavelength dependences of reflection coefficient $|R|$ and absorption A of square periodic cell arrays consisting of single rings (a) and square frames (b). A radius of medial line of the rings is 200 nm and a side size of metal frame elements is 400 nm. Ordinary dimensional resonance and maxima of transmission and reflection doublets related to excitation of second-order ordinary resonance are marked I, II and III, respectively.

The single-ring metal strip is the initial element for the concentric-rings' metal element shown in figure 2. As mentioned above, the square frame with side length 400 nm is the initial element for the elements shown in figure 3. It corresponds to the case $y_1 = y_2 = 200$ nm.

The wavelength dependences of the absolute value of the reflection coefficients $|R|$ and the normalized absorption defined as $A = 1 - |R|^2 - |T|^2$, where T is a transmission coefficient of these initial planar structures, are demonstrated in figure 5. All the resonances of both kinds of structures consisting of the gold elements are shifted from the corresponding resonances of aluminum structures to the long wavelength region. This long-wave shift is a consequence of the different wavelengths of the plasmon-polaritons that propagated along the surfaces of the aluminum and gold strip wires.

The fundamental plasmon-polariton resonances marked I (see figure 5) are the ordinary dimensional resonances. They may be observed in the wavelengths which correspond to the plasmon-polariton wavelengths λ_p , approximately the same as a circumference H of metal elements $H \approx \lambda_p$. These resonances have very wide resonance curves (Q factors are approximately 1) because of a strong coupling of the structure with a free space and an infinite substrate.

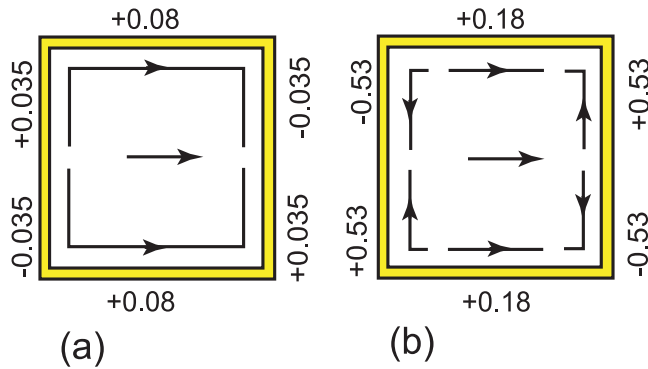


Figure 6. Schematic sketch of current distributions in a gold square frame which is an element of a planar periodic structure. The current distributions were calculated in the wavelengths of absorption maxima. Part (a) of the sketch corresponds to the ordinary dimensional resonance at a wavelength about 1800 nm. Current distribution related to second-order ordinary resonance is shown in part (b) at a wavelength of about 846 nm. Arrows and figures of the distribution scheme correspond to instantaneous direction of currents and its extreme values related to sections of the frame. The polarization of the incident wave is shown by the arrow in the center of the frame.

In order to analyze the resonance features of the arrays of narrow complex-shaped elements, it is very convenient to use current distributions. In this case we use the calculated tangential components of the electric field in metal strips as values proportional to the current density. Thus in the following, the values mentioned through sketches of the current distributions are the extremal values of the tangential component of the electric field along the medial line inside the metal strip. In short, we consider these values as the values of a current in arbitrary units.

A schematic sketch of the current distribution of the fundamental resonance by using arbitrary units is presented in figure 6(a). The current distribution was calculated in a square gold frame, which is an element of the periodic array in the absorption maximum wavelength. There are only two zeros in the current distribution. This fact shows the condition $H \approx \lambda_p$ of the fundamental resonance.

Besides the ordinary low- Q resonance, there are additional resonances (Q factors of the additional reflection resonances are approximately 13). Each of them manifests a doublet of the transmission and reflection maxima, marked II and III, respectively, in figure 5. These peaks and troughs of the reflection coefficient correspond to two neighboring wavelengths. We observe the absorption maximum in a wavelength between the wavelengths of the peak-and-trough doublet.

The sketch of the current distribution for the resonance absorption maximum (wavelength 846 nm) of the array of square gold frames is shown in figure 6(b). There are six zeros in the current distribution. Therefore, this resonance doublet corresponds to the condition $H \approx 3\lambda_p$.

There are the anti-phased currents excited along either side of the frame which is orthogonal to the electric field of the incident wave (this polarization direction is indicated by an arrow in the center of the square frame in figure 6). Within

a subwavelength periodic array, these antiparallel currents cannot radiate in free space and in the substrate. As a consequence of the low radiation losses, their amplitudes are relatively large in comparison with the amplitudes of the current components along the frame sides parallel to the polarization direction.

How are the nonradiating antiparallel components of currents excited? This is explained by the presence, in the distributions of these currents, of small sections with the currents flowing along the frame sides which are parallel to the polarization direction of the incident wave (see figure 6(b)).

Note that the current distributions in the wavelengths corresponding to the transmission (895 nm) and reflection (835 nm) peaks have the same general appearance, but the current amplitudes are smaller than the ones shown in figure 6(b). The resonance doublet of the aluminum array is beyond the boundaries of the analyzed wavelength range. At wavelengths below 750 nm, the first Floquet modes propagate from the array into the substrate almost without decaying. They essentially change the radiation conditions for the currents flowing along the square frame, destroying sharp resonances and making difficulties in the analysis of the wavelength dependences of the transmission and reflection coefficients.

The small amplitude of the second-order resonance against the fundamental plasmon-polariton resonance of the planar structure of rings (see figure 5(a)) is explained by the form of the metal elements. In this case of the array elements' geometry, the current components orthogonal to the polarization direction of the incident wave are extremely small, and the power stored by the nonradiating current components has a very small value.

One can see that there is a weak additional absorption maximum for the planar structures composed of aluminum elements in the wavelength range from 750 to 1000 nm (see figure 5). It is caused by the absorption peak of aluminum permittivity dispersion dependence (see figure 4).

It is significant that both the fundamental resonance and the second-order one discussed above are ordinary dimensional resonances. Let us suppose that we treat the same structures as the considered ones, but made from some hypothetical nondissipative materials. Then their eigenfrequencies will be complex values over radiation losses. It is the main feature that differentiates these resonances from the true trapped mode resonances with real eigenfrequencies intrinsic to nondissipative special symmetry structures composed of infinitely thin wire elements.

3.2. Trapped mode resonance in an array made up of paired concentric rings

Trapped mode resonances can exist in multielement periodic arrays. Let us first analyze the dispersion features of a fourfold-symmetry structure made up of paired concentric rings. An advantage of this high symmetry structure is its polarization insensitivity to normally incident waves.

The wavelength dependence of the absolute value of the reflection coefficient of the array of concentric aluminum rings

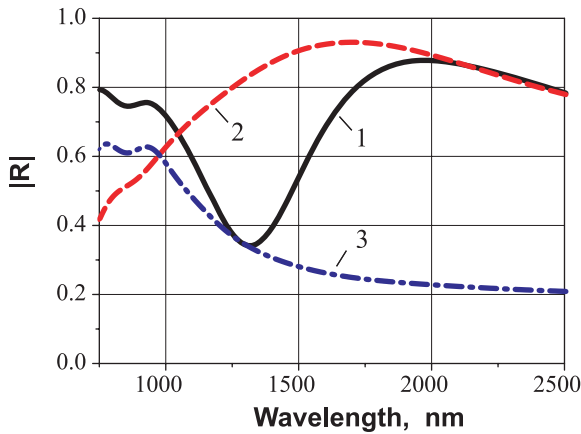


Figure 7. Wavelength dependences of reflection coefficients $|R|$ of square periodic cell arrays consisting of paired concentric aluminum rings shown in figure 2 whose radii are $r_1 = 100$ nm and $r_2 = 200$ nm (line 1), and single aluminum rings (lines 2 and 3). Lines 2 and 3 correspond to arrays of single rings which have middle radii 200 and 100 nm respectively.

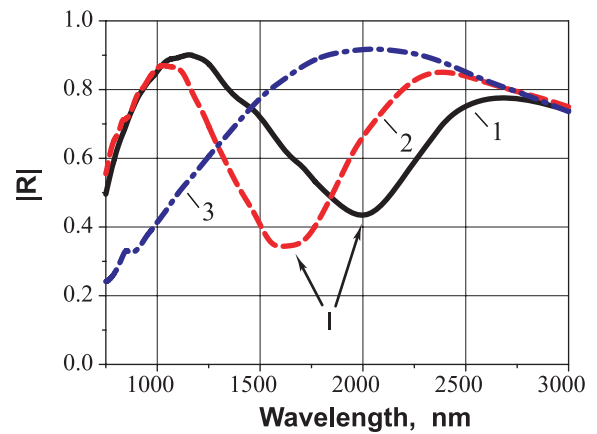


Figure 8. Wavelength dependences of reflection coefficient $|R|$ of square periodic cell arrays consisting of paired gold concentric rings shown in figure 2. The middle radius of the outer ring is $r_2 = 200$ nm. The middle radius of the inner ring has the following value: line 1— $r_1 = 120$ nm; line 2— $r_1 = 100$ nm; line 3— $r_1 = 25$ nm (in this case an inner ring degenerates into a disc).

is shown in figure 7 (line 1). The trapped mode resonance is observed as a peak of transmission (deep of reflection) breaking the fundamental reflection resonance of the planar array of initial single rings with 200 nm radius of the medial line (see line 2 in figure 7).

The trapped mode resonance arises in the wavelength range between the wavelengths of ordinary fundamental plasmon–polariton resonances of the arrays composed of single rings which make up the considered complex metal element. As a result, the resonance anti-phased currents are observed along the outer and inner rings. These currents have very weak coupling with zero Floquet modes in free space and the substrate. In this case we have an example of an isotropic polarization-insensitive structure which supports trapped mode resonance.

This resonance is inherently a true trapped mode resonance. Actually in the resonance wavelength, radiation losses of the hypothetical nondissipative structure tend to zero if r_1 tends to r_2 . Thus the imaginary part of the eigenfrequency of the array structure becomes infinitesimal. The ratio r_2/r_1 may be considered as a degree of ‘asymmetry’. The close asymmetry degree to 1 provides the higher Q factor of resonance.

Figure 8 illustrates the asymmetry degree dependence of the width and amplitude of a trapped mode resonance (marked by I). Increasing the value r_2/r_1 results in a shift of the resonance to the short wavelength range and enlargement of the resonance amplitude. Such behavior corresponds to that observed for a microwave structure with dissipative losses in the substrate [11]. There are two types of losses inherent to the structure under treatment. The first of them is radiation losses and the second one is the dissipative losses in metal. The asymmetry degree reduction results in an increase of the dissipative losses and a decrease of the radiation losses. If the inner ring degenerates to a disc (line 3 in figure 8), then the trapped mode resonance vanishes. It is explained by the impossibility of a circular current to be excited in the disc.

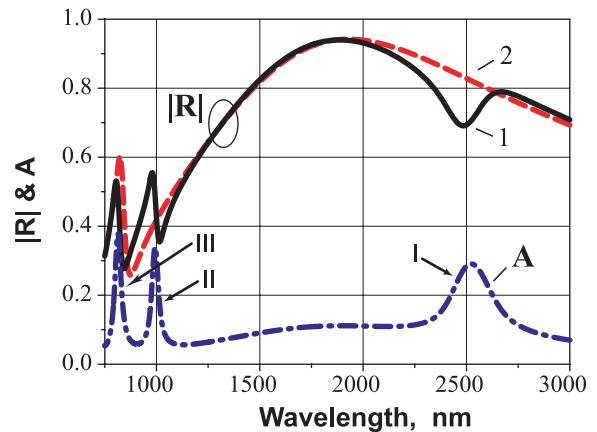


Figure 9. Wavelength dependences of reflection coefficients $|R|$ and absorption A of square periodic cell structure consisting of gold paired C-shaped elements shown in figure 3(a). Normally incident wave is linearly polarized along the x axis. Line 1 and absorption dependence correspond to structural parameters $y_1 = 150$ nm and $y_2 = 200$ nm. Line 2 concerns the structure with $y_1 = y_2 = 175$ nm.

Evidently, the array structure of concentric rings has the merit of polarization insensitivity of the response and a shortcoming of technological problems to decrease the degree of asymmetry close to 1 (the Q factor of the trapped mode resonance is only approximately 2 in our example of the array). The next point of our study is an array of broken square frames that are free from any restriction on the degree of asymmetry.

3.3. Trapped mode resonances in arrays composed of broken square frames

Very interesting data are provided via the analysis of the resonance features of a periodic structure composed of symmetrical C-shaped elements shown to be linearly polarized along the x axis. There are three absorption maxima in the investigated wavelength band (see figure 9). The first,

at the longest wavelength, is a result of a trapped mode resonance (marked by I) against the background of the ordinary fundamental plasmon–polariton reflection resonance, which is typical for the array of square frames ($H \approx \lambda_p$). The second and third absorption maxima (marked by II and III in figure 9) are placed to the right and left of the second ordinary plasmon–polariton resonance that corresponds to the condition $H \approx 3\lambda_p$. For comparison, we present the wavelength dependence of the reflection coefficient of the array structure of the symmetry broken square frames ($y_1 = y_2 = 175$ nm). It is line 2 in figure 9. This wavelength dependence of the reflection coefficient has a small displacement to the short-wavelength band, in comparison with the same dependence relative to the array of the initial square frames (see figure 5(b)). It is evident that the current distributions in such symmetry structures have no qualitative differences. This fact is also proved by the numerical simulation.

The form of the current distribution related to the first absorption maximum (figure 10(a)) demonstrates the trapped mode nature of the resonance. There are the anti-phased currents parallel to the Ox and Oy axes of the metal elements. The amplitudes of the currents flowing along sections parallel to the Ox axis are greater than those on sections along the Oy axis. Therefore the current amplitudes on short and long metal strips of the array element are not equal. This amplitude difference provides a weak coupling between the currents and the incident wave and the zero-order Floquet modes in free space and the substrate. The trapped mode resonance Q factor increases to 6 or even 11 for a structure with a small asymmetry degree.

The second absorption maximum (wavelength is about 993 nm) corresponds to a new type of trapped mode resonance. In this case the currents in all sections of the array element are anti-phased (see figure 10(b)), and there are six zeros in the current distribution. Note that this fact argues for the condition $H \approx 3\lambda_p/2$ for each metal strip. The maxima of the current amplitudes are observed in parallel to the Oy axis sections of the longer metal strip, i.e. this peculiarity of the current distribution, inherent to the array of initial square frames (figure 6(b)), remains. However, in contrast to the array of initial frames, the currents are oppositely directed in the two sections parallel to the Ox axis. Thus, the peak-and-trough reflection coefficient relative to the second absorption maximum is a high-order trapped mode resonance.

The current distribution is radically changed in the third absorption maximum (figure 10(c)). The maxima of current amplitudes are now observed in parallel to the Oy axis sections of the shorter metal strip. This fact has a simple explanation. The condition $H \approx 3\lambda_p/2$ is now fulfilled for this metal strip, while it occurred for the longer metal strip in the second absorption maximum. But it is very important that the currents parallel to the Ox axis sections are in phase now. Therefore this resonance is a higher-order ordinary plasmon–polariton resonance. Note that the reflection resonance between the ordinary trapped mode resonance (I) and the higher-order one (II) corresponds to the ordinary fundamental plasmon–polariton resonance in the symmetry structure of the initial square frames. Thus, the two ordinary

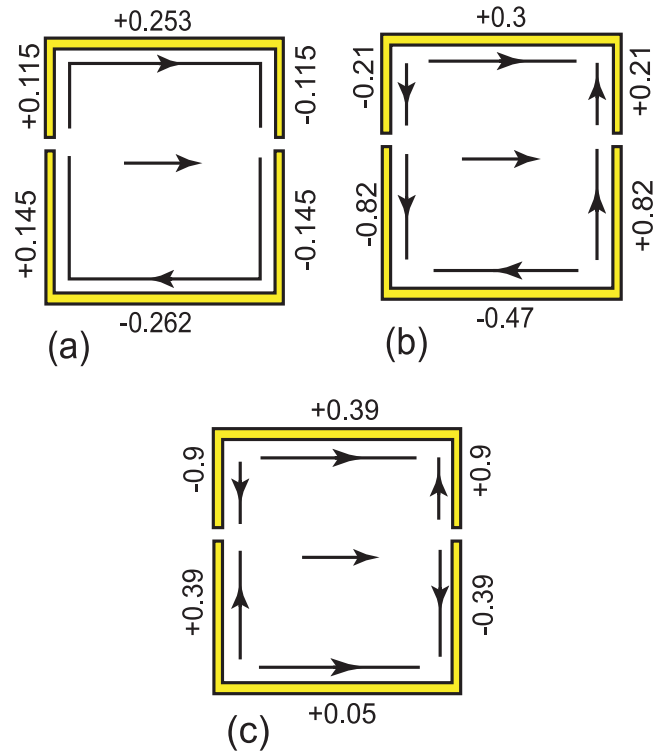


Figure 10. Schematic sketch of current distributions in asymmetry pair of C-shaped gold strips shown in figure 3(a) ($y_1 = 150$ nm and $y_2 = 200$ nm). Parts (a)–(c) of the sketch correspond to the current distribution at wavelengths of the first (2524 nm), second (993 nm) and third (813 nm) absorption maxima marked in figure 9. Arrows and figures of the distribution scheme correspond to instantaneous direction of currents and its extreme values related to sections of the complex element. The polarization of the incident wave is shown by the arrow in the center of the array element.

plasmon–polariton resonances of the symmetry structure are transformed into a pair of trapped mode resonances and a pair of ordinary plasmon–polariton resonances of the asymmetry structure (compare figures 5(b) and 9).

The asymmetry degree of paired C-shaped strips can be characterized by the ratio y_2/y_1 . The asymmetry degree dependence of the width and amplitude of the trapped mode resonances is illustrated in figure 11. Note that both trapped mode resonances are shifted towards the long-wavelength band, with the asymmetry degree increasing (see figure 11(b)), while the ordinary (fundamental and second-order) plasmon–polariton resonances are shifted towards the short-wavelength band. As mentioned above, the trapped mode resonances are excited if the currents in the parallel sections of the array element are anti-phase. In this case, increasing the longer metal strip length results in a long-wavelength shift of the trapped mode resonances. The ordinary plasmon–polariton resonances require co-phased currents, which results in this resonance wavelength being brought into correlation with the smaller metal strip length. Thus, if the smaller metal strip length is decreasing, then these resonances are shifted to the short-wavelength range.

One can see that the third absorption maximum leaves the wavelength range under investigation with an increasing asymmetry of the structure.

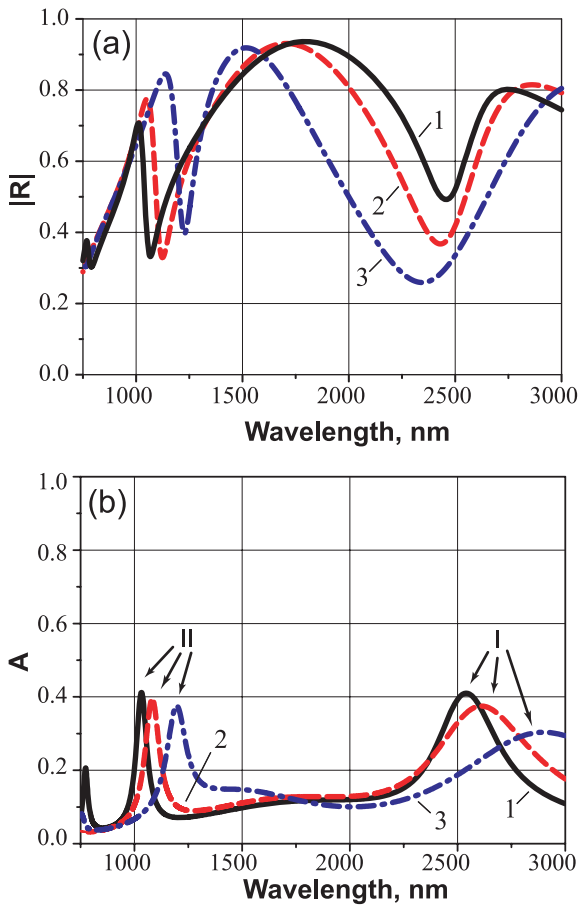


Figure 11. Wavelength dependences of reflection coefficient $|R|$ (a) and absorption A (b) of periodic structure consisted of elements shown in figure 3(a). The normally incident wave has x polarization. Geometry parameters of the gold elements are as follows: line 1— $y_1 = 125$ nm and $y_2 = 225$ nm, line 2— $y_1 = 100$ nm and $y_2 = 250$ nm, and 3— $y_1 = 50$ nm and $y_2 = 300$ nm.

An essential difference of features between of the first and the second trapped mode resonances is observed in accordance with the structure asymmetry degree. If the structure asymmetry increases, the wavelength width between the reflection peak and trough relative to the first trapped mode resonance also increases. At the same time, the wavelength width of the reflection peak-and-trough of the second high-order trapped mode resonance is almost constant. Such resonance behavior is directly related to the trapped mode excitation condition. Excitation of the trapped mode resonances of a planar array of aluminum elements is illustrated in figure 12. A complex element of the array consists of a C-shaped strip and dipole, i.e. a linear segment of the strip. In this case, the ordinary trapped mode resonance is excited in the wavelength region between the fundamental plasmon-polariton resonances of the array of single C-shaped elements and the array of single dipoles. The condition $H \approx \lambda_p/2$ corresponds to this resonance excitation.

The second trapped mode resonance is excited in the wavelength range bounded by conditions $H \approx 3\lambda_p/2$ and $H \approx \lambda_p/2$ of the ordinary plasmon-polariton excitation in the array of single C-shaped elements and the array of single dipole elements, respectively.

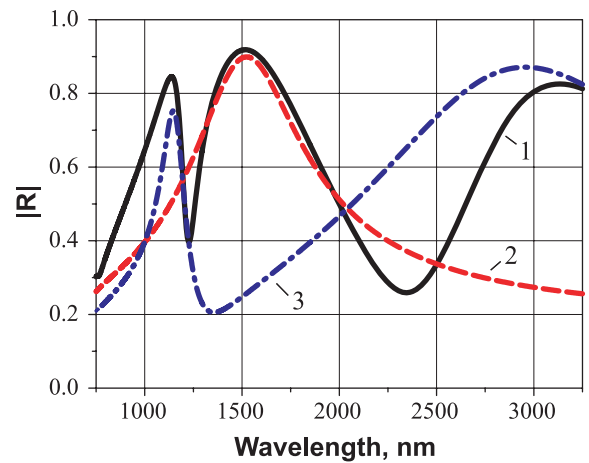


Figure 12. Wavelength dependences of reflection coefficient $|R|$ of x -polarized wave for the periodic structure with aluminum elements. Line 1 corresponds to the array of elements shown in figure 3(a) with parameters $y_1 = 50$ nm and $y_2 = 300$ nm. Lines 2 and 3 are related to the array of single C-shaped elements ($y_2 = 300$ nm) and the array of dipoles ($y_1 = 50$ nm), respectively.

Thus we can assert that the $H \approx 3\lambda_p$ plasmon-polariton resonance of the initial square frame structure transforms into the asymmetry structure resonance which corresponds to the $H \approx 2\lambda_p$ condition. The wavelength of such a resonance is larger than the wavelength of the initial plasmon-polariton resonance. Thus in our case, an increasing y_2/y_1 ratio results in a widening of the wavelength band between the ordinary plasmon-polariton resonances, and, as a result, the maxima of transmission and reflection of the first trapped mode resonance doublet are shifted in opposite directions.

As concerns the second trapped mode resonance, it changes the current distribution which corresponds to a gradual transformation of the $H \approx 3\lambda_p$ ordinary plasmon-polariton resonance of the symmetry structure to the $H \approx 2\lambda_p$ ordinary plasmon-polariton resonance of the asymmetry structure, and both the peak and trough of the reflection are shifted to the long-wavelength range.

Finally let us consider excitation of the second-order trapped mode resonance under the assumption that $H \approx 3\lambda_p/2$ and $H \approx \lambda_p/2$ reflection resonances of a C-shaped strip and strip dipole, respectively, are overlapped. With that end in view, we calculated the wavelength dependences of the reflection coefficient of the array of elements in figure 3(a) with sizes $y_1 = 50$ nm and $y_2 = 300$ nm, and two arrays of the same kind but with a reduced dipole length. For a wavelength of about 1250 nm, one can see in figure 13 a sharp trough in the reflection coefficient caused by the second-order trapped mode excitation. The Q factor of the transmission peak corresponded to the second-order trapped mode resonance increases to 26 for such a geometry. It is twice as much as the Q factor of the second-order ordinary plasmon-polariton resonance of the symmetrical structure. Let us note that further decreasing of the dipole length results in the disappearance of the main trapped mode resonance, which corresponds to the condition $H \approx \lambda_p/2$ for both metal strips.

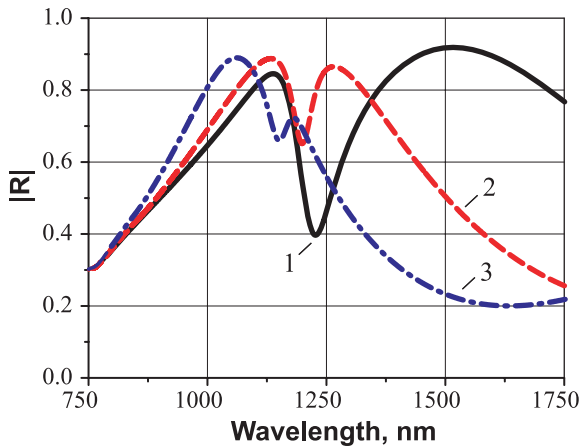


Figure 13. Wavelength dependences of reflection coefficient of a square cell periodic structure. Complex gold element of the periodic cell includes a C-shaped strip and strip dipole. Line 1 corresponds to the array of elements shown in figure 3(a) with sizes $y_2 = 300$ nm and $y_1 = 50$ nm (in this case the length of the dipole is 400 nm). Lines 2 and 3 correspond to lengths of dipole 300 and 250 nm. The incident wave is polarized along the Ox axis.

The periodic structure composed of the elements in figure 3(b) has a typical trapped mode resonance near a wavelength corresponding to the condition $H \approx m\lambda_p/2$ ($m = 1, 3, 5, \dots$) for single C-shaped parts of these complex elements (see figure 14, the trapped mode resonance is marked by I). Such a plasmon-polariton resonance should not be excited in the symmetry structure because of specific current distribution. There are the anti-phased currents in the metal element sections parallel to the Oy axis. In contrast to the above considered structure, the trapped mode resonance corresponds to a reflection peak and it is excited only by the y -polarized incident wave which has an electric field directed orthogonal to the symmetry axis of the metal strips. The ordinary plasmon-polariton resonance corresponds to the $H \approx m\lambda_p$ ($m = 1, 2, 3, \dots$) condition. The Q factor of the fundamental ordinary plasmon-polariton resonance has a value from 2 to 3 and the fundamental trapped mode resonance Q factor is approximately 9.

The asymmetry degree (y_2/y_1) dependences of amplitude and Q factor of the trapped mode resonance demonstrate the same behavior as in the case of the array of a pair of concentric rings. Let us note that the dissipative losses in the metal result in destroying the high- Q resonances whose excitation could be expected in the structure with weakly asymmetry metal elements, i.e. $y_1 \approx y_2$. In fact these resonances are accompanied by high amplitude currents and, as a result, high energy dissipation in the metal.

There are two additional reflection resonances for the structure from gold elements in the considered wavelength band (750–3000 nm). One of them is the second-order ordinary plasmon-polariton resonance (it corresponds to the $H \approx 2\lambda_p$ condition for a single metal strip). The second resonance is the second-order trapped mode resonance. The last one corresponds to the $H \approx 3\lambda_p/2$ condition and has a very weak coupling with the free space and substrate. The amplitude of the second trapped mode resonance is less than 0.1% of the

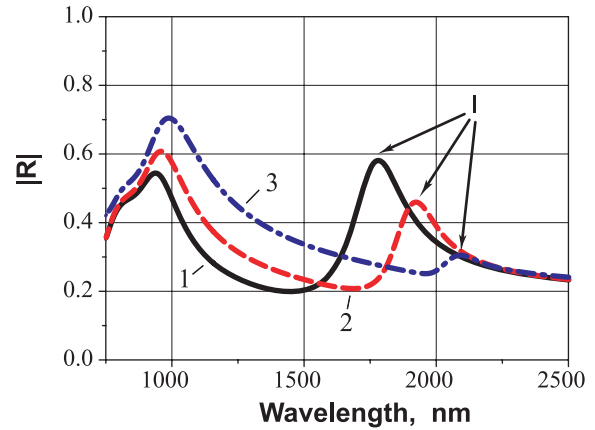


Figure 14. Wavelength dependences of reflection coefficient $|R|$ of a planar periodic structure consisting of aluminum elements shown in figure 3(b). Normally incident wave has y polarization. Besides the general geometric parameters of a periodic cell mentioned above, the rest of the sizes of the elements are chosen as follows: $y_2 = 175$ nm; line 1— $y_1 = 50$ nm, line 2— $y_1 = 100$ nm, line 3— $y_1 = 150$ nm.

total reflection level for all considered values of asymmetry degree (y_2/y_1). However, the values of the current amplitudes excited in the metal strips are at least three times greater for the second-order resonances than those in the case of the fundamental resonances.

3.4. Trapped mode resonances in slit arrays complementary to the strip structures

Another practical topic of trapped mode resonance studies relates to features of these resonances in the complementary slits-in-screen structures, particularly in light of the impressive experimental observations presented in [15].

Let us now consider a periodic structure in the form of a slit array which is complementary to the strip structure shown in figure 3(a). In this case a periodic array of complex slits is cut in a planar metal layer placed on a semi-infinite silica substrate. We assume that the metal of the layer is gold or aluminum and is 50 nm thick. All slits of the array have the same width, 50 nm.

On the grounds of the Babinet principle, one can expect that the transmission coefficient wavelength dependence of the slit structure excited by a y -polarized incident wave will be the same as the reflection one of the complimentary strip structure excited by an x -polarized wave. However, we can assert only that there is some qualitative correspondence in the considered problems. Actually, in the strict sense, the Babinet principle is applicable to the problems of electromagnetic wave scattering by infinitely thin perfect conducting complimentary screens in an isotropic homogeneous space [23]. In the treated problem, the metal layer has a finite thickness and is placed on a substrate, and in the near-IR region its electrical properties substantially differ from those of a perfect conducting screen. Thus, a direct study of the resonance properties of slit structures is needed.

Wavelength dependences of the transmission coefficient and absorption are shown in figure 15 for the structures

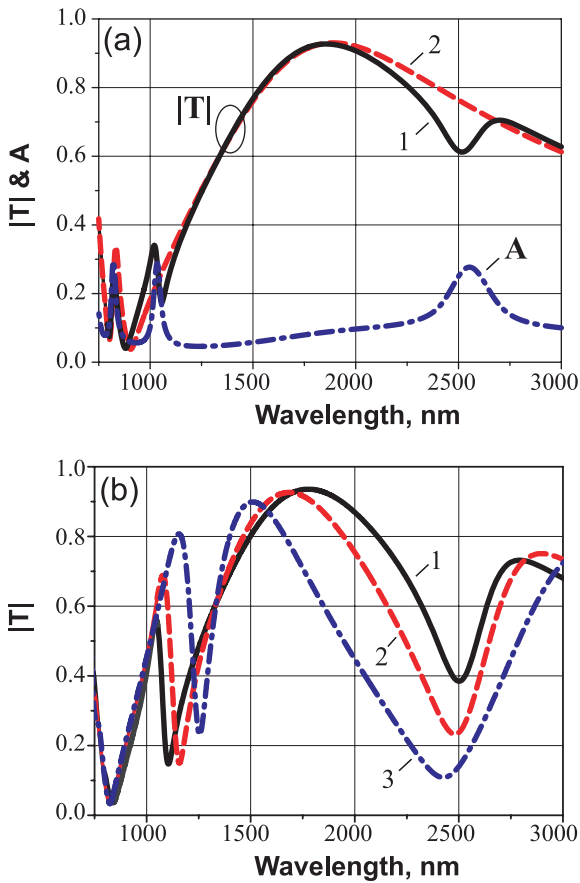


Figure 15. Wavelength dependences of the transmission coefficient $|T|$ and the absorption one (line A in part (a)) of the y -polarized wave of the periodic structure with paired C-shaped slits in gold layer. The dependences presented in parts (a) and (b) were calculated for the complementary structures with respect to the strip structures whose reflection and absorption features are illustrated in figures 9 and 11(a), respectively.

complementary to the structures whose transmission and absorption are presented in figures 9 and 11. One can see a good agreement between the transmission coefficient of the slit structure (figure 15) and the reflection coefficients of the strip structure (figures 9 and 11). Thus in our case, the Babinet principle provides a good prediction of results. As was shown by numerical simulations, the ‘magnetic current’ distributions relative to the three absorption maxima (see figure 15(a)) of the slit structure coincide with the current distributions of the strip structure.

3.5. Array structure with a finite thickness substrate

Essentially, let us return to the question of the difference between the reflection and transmission properties of an array placed on a semi-infinite and on a practical finite thickness substrate.

The effect of the finite thickness of the substrate on the wavelength dependence of the reflection coefficients of the structure is illustrated in figure 16. A large wave thickness of any practical substrate (of about 0.5 mm) results in the appearance of a large number of interference resonances

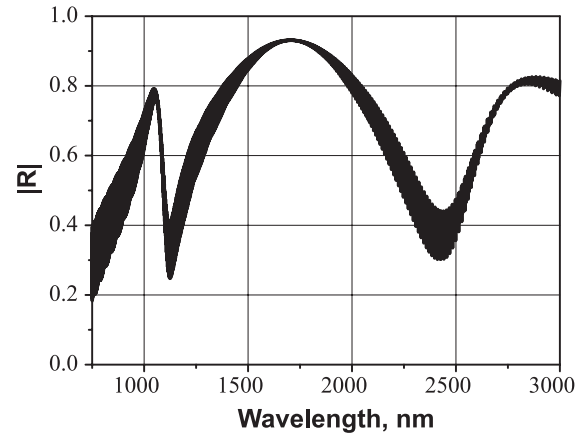


Figure 16. Wavelength dependence of reflection coefficient of x -polarized wave of a gold strip periodic structure with elements shown in figure 3(a). Graph resolution is not enough for the strong interference oscillations and they are seen as a wide line. Structural sizes are $y_1 = 100$ nm and $y_2 = 250$ nm, and thickness of the substrate is $L = 0.5$ mm.

masking the trapped mode resonances. However, some averaged line of the wavelength dependence has a good agreement with the reflection coefficient of the structure with an infinite substrate (please compare line 2 in figure 11(a) with that in figure 16).

4. Conclusions

The problem of near-IR light reflection from and transmittance through a planar 2D metal–dielectric array structure with a square periodic cell consisting of two complex-shaped asymmetric metal elements has been solved. We show that a small degree of asymmetry of such structures reveals trapped mode resonances. The true trapped mode resonance is a resonance with the real eigenfrequency intrinsic to the special symmetry hypothetical nondissipative open structures particularly composed of thin wire elements. Anti-phased currents of parallel sections of the metal elements are inherent to such resonances. It results in a weak coupling between the currents and zero Floquet modes in a free space and a substrate.

The conditions of light confinement by an excitation of the trapped mode resonances of some kinds of structures both polarization-sensitive and -insensitive were studied. It was shown that, if the complex metal element of an array is composed of two unequal length metal strips, the trapped mode resonance arises in the wavelength range between the wavelengths of the ordinary plasmon–polariton resonances of arrays consisting of single metal strips. In contrast, the trapped mode resonance of a structure composed of elements with two equal length metal strips arises at the wavelength of the stopped ordinary plasmon–polariton resonances of arrays of single metal strips.

As shown in our study, two factors restrict a trapped mode resonance Q factor. They demonstrate an opposite dependence on the structural asymmetry degree. The first factor is currents coupling with zero Floquet modes in the substrate and free space and the second one is Joule losses

increasing on decreasing the structural asymmetry degree. However, the special choice of geometry parameters of the structure enables us to increase the Q factor of the trapped mode resonance by several times in comparison with the ordinary plasmon–polariton resonance. For example, the fundamental trapped mode resonance Q factor is varied from 2 to 11 for the structures considered in this paper, while the value of the fundamental plasmon–polariton resonance Q factor is approximately 1.

For the first time we show the existence of a high-order trapped mode resonance with a greater quality factor than the quality factor of the lowest one. In our calculations we observe that the Q factor of the high-order trapped mode resonance reaches 30 for real structures.

The trapped mode resonances are accompanied by relatively high values of the electric field in and around the metal strips (or slits in the metal layer of a complementary structure). Thus use of the planar structure with the ‘trapped mode’ resonance in infrared and optical ranges is very useful. In fact, we observe an effect of light trapping by the metal arrays with a high level of IR power stored in localized field states of a discrete spectrum. This opens intriguing perspectives of such regime application in structures with lasing materials and in arrays with nonlinear inclusions.

It was ascertained also that the Babinet principle provides a good prediction of resonance properties of the complementary structures in spite of very high Joule losses in metals in the near-IR region, the finite thickness of metal elements and the presence of a dielectric substrate.

Acknowledgment

The authors would like to acknowledge the partial financial support provided by the National Academy of Sciences of Ukraine (grant no. 1-02-a).

References

- [1] Munk B A 2000 *Frequency Selective Surfaces: Theory and Design* (New York: Wiley)
- [2] Smith D R, Pendry J B and Wiltshire M C K 2004 Metamaterials and negative refractive index *Science* **305** 788–92
- [3] Fedotov V A, Mladyonov P L, Prosvirnin S L, Rogacheva A V, Chen Y and Zheludev N I 2006 Asymmetric propagation of electromagnetic waves through a planar chiral structure *Phys. Rev. Lett.* **97** 167401
- [4] Fedotov V A, Schwanecke A S, Zheludev N I, Khardikov V V and Prosvirnin S L 2007 Asymmetric transmission of light and enantiomerically sensitive plasmon resonance in planar chiral nanostructures *Nano Lett.* **7** 1996–9
- [5] Fedotov V A, Mladyonov P L, Prosvirnin S L and Zheludev N I 2005 Planar electromagnetic metamaterial with a fish scale structure *Phys. Rev. E* **72** 056613(4)
- [6] Schwanecke A S, Fedotov V A, Khardikov V V, Prosvirnin S L, Chen Y and Zheludev N I 2007 Optical magnetic mirrors *J. Opt. A: Pure Appl. Opt.* **9** L1–2
- [7] Schurig D *et al* 2006 Metamaterial electromagnetic cloak at microwave frequencies *Science* **314** 977–80
- [8] Prosvirnin S L and Zouhdi S 2001 Multi-layered arrays of conducting strips: switchable photonic band gap structures *Int. J. Electron. Commun. (AEÜ)* **55** 260–5
- [9] Prosvirnin S and Zouhdi S 2003 Resonances of closed modes in thin arrays of complex particles *Advances in Electromagnetics of Complex Media and Metamaterials* ed S Zouhdi *et al* (Dordrecht: Kluwer Academic) pp 281–90
- [10] Blackburn J F and Arnaut L R 2004 High performance split ring FSS for WLAN bands *Proc. 27th ESA Antenna Technology Workshop on Innovative Periodic Antennas: Electromagnetic Bandgap, Left-handed Material, Fractal and Frequency Selective Surfaces* (Santiago de Compostela: European Space Agency) pp 329–36
- [11] Fedotov V A, Rose M, Prosvirnin S L, Papasimakis N and Zheludev N I 2007 Sharp trapped-mode resonances in planar metamaterials with a broken structural symmetry *Phys. Rev. Lett.* **99** 147401
- [12] Hill R A and Munk B A 1996 The effect of perturbing a frequency-selective surface and its relation to the design of a dual-band surface *IEEE Trans. Antennas Propag.* **44** 368–74
- [13] Fano U 1961 Effects of configuration interaction on intensities and phase shifts *Phys. Rev.* **124** 1866–78
- [14] Zheludev N I, Prosvirnin S L, Papasimakis N and Fedotov V A 2008 Lasing spacer *Nat. Photon.* **2** 351–4
- [15] Plum E, Fedotov V A, Kuo P, Tsai D P and Zheludev N I 2009 Towards the lasing spacer: controlling metamaterial optical response with semiconductor quantum dots *Opt. Express* **17** 8548–51
- [16] Gao X, Mirotznik M S, Shi S and Prather D W 2004 Applying a mapped pseudospectral time-domain method in simulating diffractive optical elements *J. Opt. Soc. Am. A* **21** 777
- [17] Khardikov V V, Iarko E O and Prosvirnin S L 2008 Using transmission matrix and pseudospectral time-domain method to study of light diffraction on planar periodic structures *Radiophys. Radioastron.* **13** (2) 146–58
- [18] Khardikov V V, Yarko E O and Prosvirnin S L 2007 Fast algorithm for solving of the light diffraction problem on planar periodic structures *Proc. 12th Int. Conf. on Seminar/Workshop on Direct and Inverse Problems of Electromagnetic and Acoustic Wave Theory (Lviv)* pp 73–6
- [19] Taflove A and Hagness S C 2005 *Computational Electrodynamics: The Finite-Difference Time-Domain Method* (Boston, MA: Artech House)
- [20] Han M, Durrón R W and Fan S 2006 Model dispersive media in finite-difference time-domain method with complex-conjugate pole-residue pairs *IEEE Microw. Wirel. Compon. Lett.* **16** 119–21
- [21] Vial A and Laroche T 2008 Comparison of gold and silver dispersion laws suitable for FDTD simulations *Appl. Phys. B* **93** 139–43
- [22] http://www.mellesgriot.com/products/optics/mp_3_2.htm
- [23] Jackson J D 1999 *Classical Electrodynamics* 3rd edn (New York: Wiley)